Substantial energy input to the mesopelagic ecosystem from the seasonal mixed-layer pump

Giorgio Dall'Olmo[1,2,3], James Dingle[1], Luca Polimene[1], Robert J.W. Brewin[1,2], Hervé Claustre[4,5]

[1] *Plymouth Marine Laboratory, UK*
[2] *National Centre for Earth Observations, Plymouth Marine Laboratory, UK*
[3] *Hjort Centre for Marine Ecosystem Dynamics, Bergen, Norway*
[4] *UPMC Univ Paris 06, UMR 7093, Laboratoire d'Océanographie de Villefranche, 06230 Villefranche-sur-Mer, France*
[5] *CNRS, UMR 7093, LOV, 06230 Villefranche-sur-Mer, France*

Supplementary Materials

Supplementary Discussion

Traditional sampling methods cannot detect the mixed-layer pump. To detect the flux driven by the seasonal mixed-layer pump two criteria need to be simultaneously met by in-situ methods. First, data at sufficiently high temporal resolution are needed to sample the rapid transition between the deepest mixed layer and summer stratification. Second, the method should be able to detect the redistribution of slowly-sinking organic matter in the water column. To the best of our knowledge, rarely have these two conditions been simultaneously fulfilled when measuring carbon export with traditional methodologies.

The most common methods to measure the export flux rely on detecting a signal that is generated by particles sinking below the upper-ocean productive layer and make use of sediment traps (moored to the sea floor, surface tethered, or neutrally buoyant)[1] or the ^{234}Th:^{238}U disequilibrium[2]. Neutrally buoyant sediment traps are designed to sample in Lagrangian mode (i.e., by following water parcels) to minimise hydrodynamic biases[3]. Often they are programmed to follow isopycnals and to sample for a few (1-6) days[4]. Likely because of the strong vertical mixing typical of the end of the winter, these traps have not been deployed in regions with deep mixed layers during the formation of the summer stratification. Thus, it is unlikely that current export data from NBSTs can be used to quantify the mixed-layer pump. The export flux driven by the mixed-layer pump would also be undersampled by deep (>1000 m) moored sediment traps, because the slowly-settling particles would likely be remineralised before being collected, unless these particles aggregated and rapidly sank after the establishment of the summer stratification[5]. The ^{234}Th:^{238}U disequilibrium method relies on the vertical separation that is established between the particle-refractory ^{238}U and the reactive ^{234}Th, when the latter is adsorbed onto sinking particles and removed from the ocean surface. Most of the particles driving the mixed layer pump, however, are slowly-sinking and would not create an appreciable vertical separation during the transition from the deepest mixed layer and the summer stratification. Thus, it is unlikely that the ^{234}Th:^{238}U disequilibrium method can quantify the export generated by the mixed-layer pump. In summary, all methods that rely on detecting a flux of sinking particles seem inappropriate to observe the mixed-layer pump. Data from the above methods have been used to calibrate/validate current estimates of global carbon export[6,7]. We thus conclude that these estimates are not including the contribution of the mixed-layer pump.

One of the most reliable techniques to detect the signal of the mixed-layer pump in-situ is building a biogeochemical budget. Indeed, regional studies based on biogeochemical budgets have detected the presence of the mixed-layer pump for more than twenty years[5,8,9].

Satellite estimates of particulate organic carbon (POC). Figure S2 presents the distributions of POC estimates at the time of the deepest mixed layer (t_{max}) and of stratification (t_{strat}). These estimates are typical for the start of the growing season in regions with winter mixed layers deeper than 100 m (e.g., 10, 11) and within the range of POC values used to calibrate satellite algorithms[12,13]. This comparison supports our estimates of POC from space. In addition, validation studies have already been conducted using independent collocated in-situ and satellite POC data and have demonstrated that satellite POC estimates are affected by relative uncertainties of about 50%[14,15].

Estimating POC stocks from surface POC values. An important assumption in our calculations is that the POC estimated by satellites can be exploited to predict the POC stock in the entire mixed layer. Ocean-colour satellite sensors detect light reflected within the first optical depth of the water column, which can reach maximum values of 50 m in the clearest waters[16]. Because our analysis focuses on regions of the ocean where mixed layers are deeper than 100 m and can reach values as deep as 700 m (Figure S5), it is critical to demonstrate that POC is homogeneous within the mixed layer.

To ensure that this assumption is verified, we started by selecting a conservative estimate of mixed-layer depth[17] (see Methods section).

Because, in-situ POC profiles in high-latitude regions before the time of summer stratification are scarce, we employed particulate optical backscattering data collected by instruments mounted on autonomous BioArgo floats to test our hypothesis that particles are homogeneously distributed in the mixed layer (as estimated by the Holte and Talley, 2009, algorithm). Particulate optical backscattering is commonly used as proxy of particulate organic carbon[18,19].

We analysed data from 90 BioArgo floats hosted by the Laboratoire d'Oceanographie de Villefranche (http://www.oao.obs-vlfr.fr/bioargo/summary.html). After excluding all profiles for which the Holte and Talley density-based mixed layer estimate was shallower than 100 m, 800 profiles remained which were distributed between latitudes spanning from 63°S to 70°N. For each of these profiles, we computed the ratio of the median value of the particulate optical backscattering between 10 and 20 metres,

b_{bp}(surf), and its median value in the entire mixed layer, $b_{bp}(z_m)$. Figure S4 demonstrates that the distribution of this ratio is centred on a mean value of 1.01 with a standard deviation of 0.12. We thus conclude that, as hypothesized, we can exploit surface POC estimates to predict POC stocks in the mixed layer.

Supplementary Table 1: Median relative variations in E_{tot} for corresponding relative variations in the variables used for its estimation. t_{strat} did not have any significant effect and is thus not reported.

Input variable	**Relative variation in input variable**	**Relative variation in E_{tot}**
POC	0.5, 2.0	0.5, 2.0
z_m	0.7, 1.3	0.7, 1.3

Additional references used in the Supplementary Discussion

1. Andrew M.P. et al. The oceanographic toolbox for the collection of sinking and suspended marine particles. *Progr. Oceanogr.* **133,** 17-31 (2015).

2. Buesseler, K. O. et al. Carbon and nitrogen export during the JGOFS North Atlantic Bloom Experiment estimated from 234Th, 238U disequilibria. *Deep-sea Res.* **39,** 1115-1137 (1992).

3. Buesseler, K. O. et al. An assessment of the use of sediment traps for estimating upper ocean particle fluxes. *J. Mar. Res.* **65,** 345-416 (2007).

4. Martin, P. et al. Export and mesopelagic particle flux during a North Atlantic spring diatom bloom. *Deep-sea Res. Pt. I* **58,** 338-349 (2011).

5. Körtzinger, A. et al. The seasonal pCO(2) cycle at 49 degrees N/16.5 degrees W in the northeastern Atlantic Ocean and what it tells us about biological productivity. *J. Geophys. Res. Oceans* **113,** C04020 (2008).

6. Siegel, D. A. et al. Global assessment of ocean carbon export by combining satellite observations and food-web models. *Global Biogeochem. Cy.* **28,** 2013GB004743 (2014).

7. Buesseler, K. O. et al. Revisiting carbon flux through the ocean's twilight zone. *Science* **316,** 567--570 (2007).

8. Koeve, W. Wintertime nutrients in the North Atlantic - New approaches and implications for new production estimates. *Mar. Chem.* **74,** 245-260 (2001).

9. Garside, C. and Garside, J. C., The f-ratio on 20-degrees-w during the north-Atlantic bloom experiment. *Deep-sea Res. Pt. II* **40,** 75-90 (1993).

10. Lomas, M.W. et al. Two decades and counting: 24-years of sustained open ocean biogeochemical measurements in the Sargasso Sea. *Deep-sea Res. Pt. I* **93,** 16-32 (2013).

11. Stramski, D. et al. Relationships between the surface concentration of particulate organic carbon and optical properties in the eastern South Pacific and eastern Atlantic Oceans. *Biogeosciences* **5,** 171-201 (2008).

12. Allison, D. B. and Stramski, D. and Mitchell, B. G., Empirical ocean color algorithms for estimating particulate organic carbon in the Southern Ocean. *J. Geophys. Res.* **115,** C10044 (2010).

13. Duforet-Gaurier, L. et al. Estimates of particulate organic carbon over the euphotic depth from in situ measurements. Application to satellite data over the global ocean. *Deep-sea Res. Pt. I* **57,** 351-367 (2010).

14. Świrgoń, M. and Stramska, M. Comparison of in situ and satellite ocean color determinations of particulate organic carbon concentration in the global ocean. *Oceanologia* **57,** 25-31 (2015).

15. Gordon, H. R. and McCluney, W. R. Estimation of the Depth of Sunlight Penetration in the Sea for Remote Sensing. *Appl. Optics* **14,** 413-416 (1975).

16. Holte, J. and Talley, L. A new algorithm for finding mixed layer depths with applications to argo data and subantarctic mode water formation. *J. Atmos. Oceanic Technol.* **26,** 1920-1939 (2009).

17. Stramski, D. et al. Estimation of particulate organic carbon in the ocean from satellite remote sensing. *Science* **285,** 239-242 (1999).

18. Cetinic, I. et al. Particulate organic carbon and inherent optical properties during 2008 North Atlantic Bloom Experiment. *J. Geophys. Res.* **117,** C06028 (2012).

Extended Data Figures

Figure S1: **Winter mixed layers and carbon fluxes by the seasonal mixed-layer pump.** Spatial distribution and magnitude of winter mixed layers (z_{max}, **a**) and estimates of particulate organic carbon export by the mixed-layer pump (E_{tot}, **b**). Light grey colour indicates regions for which either z_{max}<100 m (e.g., equatorial regions) or for which no data were available (e.g., seasonally ice-covered polar regions).

Figure S2: **Estimated POC.** Frequency distribution of the POC estimates at the time of the deepest mixed layer (**a**) and at the time of stratification (**b**).

Figure S3**: Data availability.** Frequency distribution of in-situ Argo observations used in the analysis as a function of time.

Figure S4: **The particulate organic carbon in the mixed layer can be estimated from its value at the surface.** Frequency distribution of the ratio of median particulate optical backscattering between 10 and 20 m, b_{bp}(surf), to the median particulate optical backscattering within the mixed layer, $b_{bp}(z_{\mathrm{m}})$. Mixed-layer depth, z_{m}, was estimated with the density algorithm proposed by Holte and Talley (2009). To prepare this plot we analysed data from 800 Bio-Argo profiles with mixed-layer depths deeper than 100 m.

Figure S5**: E_{tot} vs. z_{max}.** Parametrization of annual particulate carbon export by the mixed-layer pump (E_{tot}) as a function of winter mixed layer depth (z_{max}).

Figure S6: **Δt.** Frequency distribution of Δt, the number of days between the deepest winter mixed layer and the time when the summer stratification is established.

Figure S7: **Spatial distribution and magnitude of the contribution to the export of the mixed-layer pump by background particles present in the mesopelagic prior to the formation of the deepest mixed layer.** Values of E_{bck}:E_{tot} were obtained by analysing data from profiling floats mounting optical backscattering sensors that can be used to estimate POC.

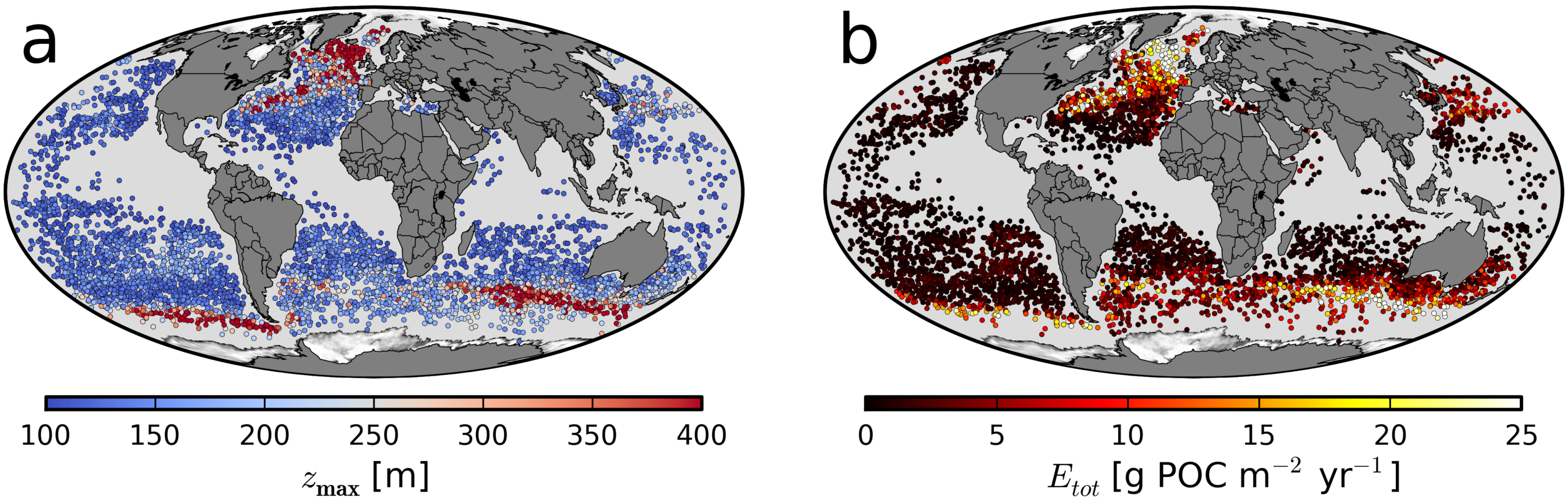
a
100
150
200
250
300
350
400
$z_{\mathbf{max}}$ [m]
b
0
5
10
15
20
25
E_{tot} [g POC m^{-2} yr^{-1}]

Figure S1

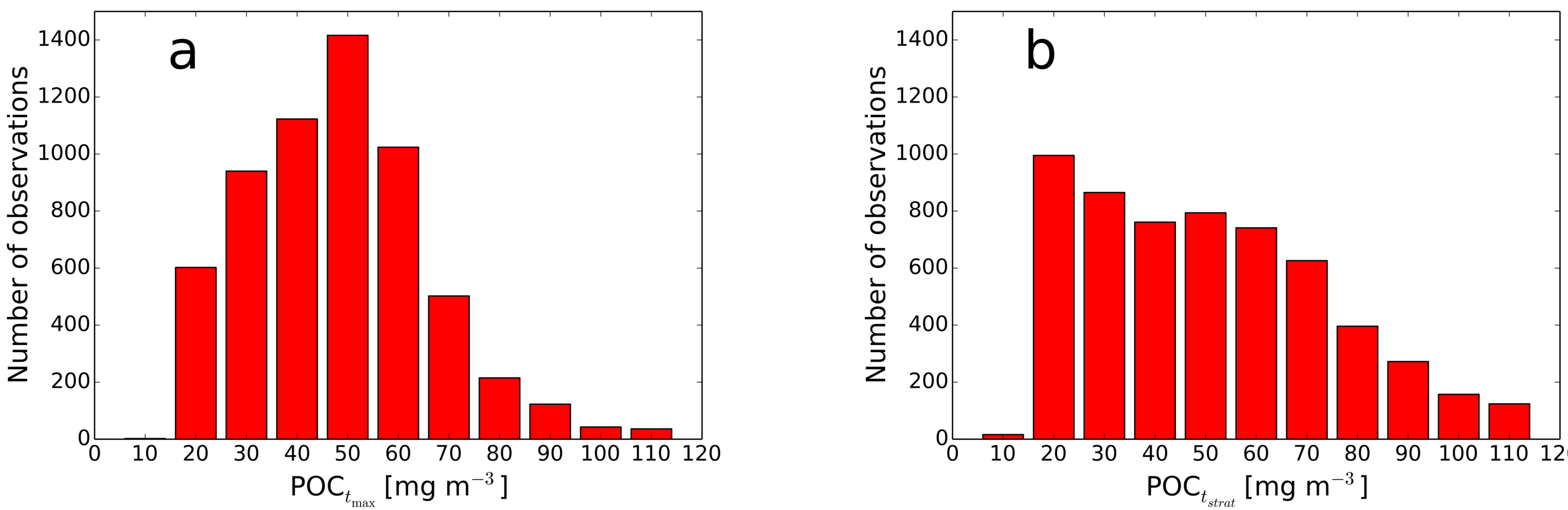
a
Number of observations
0
200
400
600
800
1000
1200
1400
0 10 20 30 40 50 60 70 80 90 100 110 120
POC$_{t_{\max}}$ [mg m^{-3}]
b
Number of observations
0
200
400
600
800
1000
1200
1400
0 10 20 30 40 50 60 70 80 90 100 110 120
POC$_{t_{strat}}$ [mg m^{-3}]

Figure S2

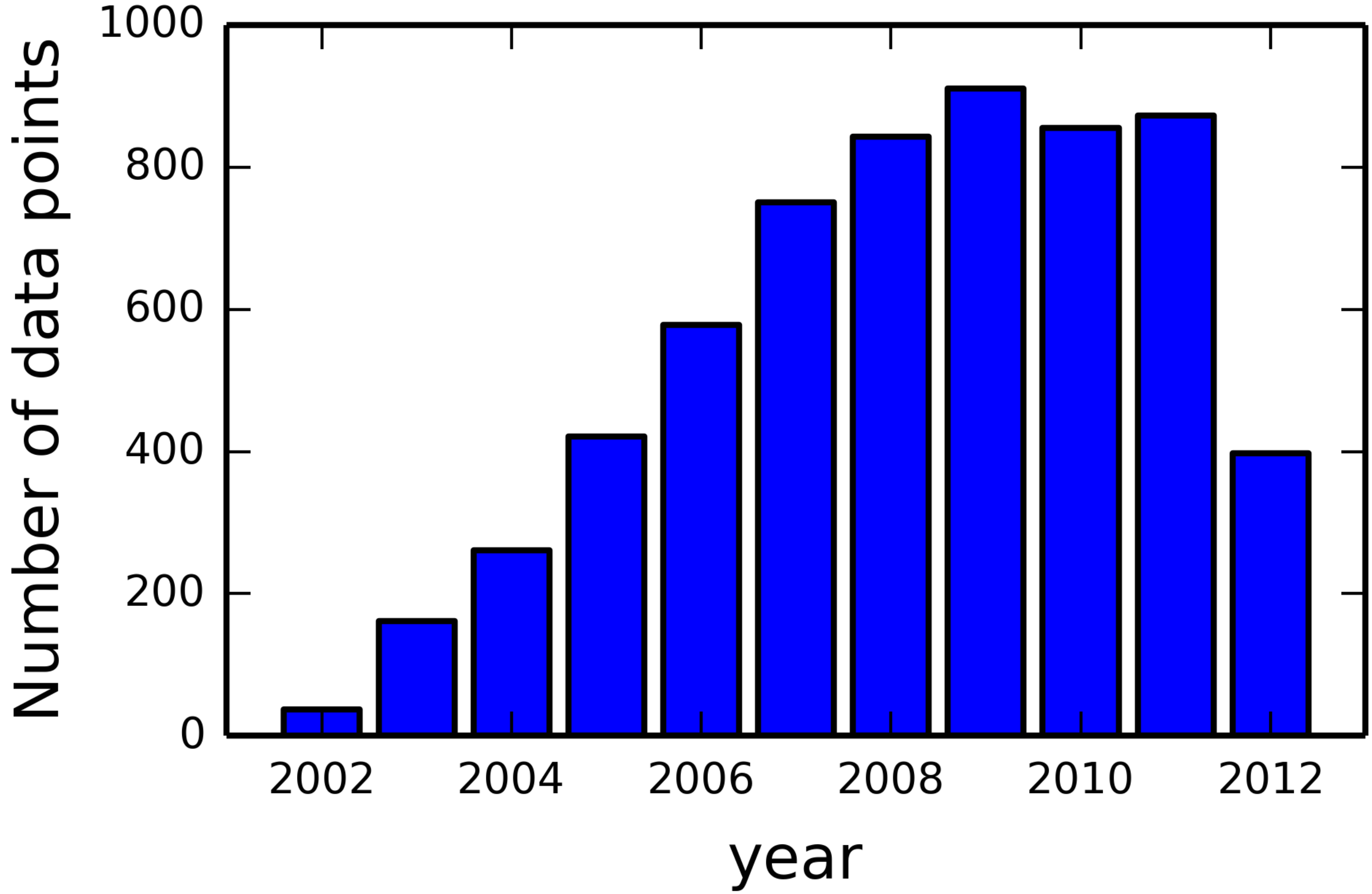
1000
800
600
400
200
0
Number of data points
2002
2004
2006
2008
2010
2012
year

Figure S3

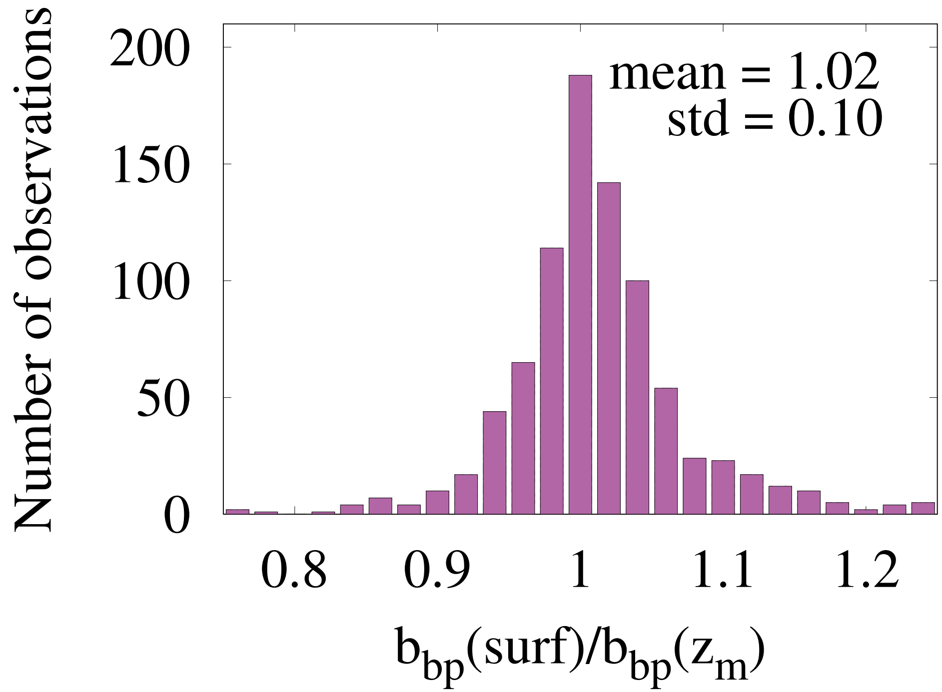

Number of observations
200
150
100
50
0
mean = 1.02
std = 0.10
0.8
0.9
1
1.1
1.2
$b_{bp}(surf)/b_{bp}(z_m)$

Figure S4

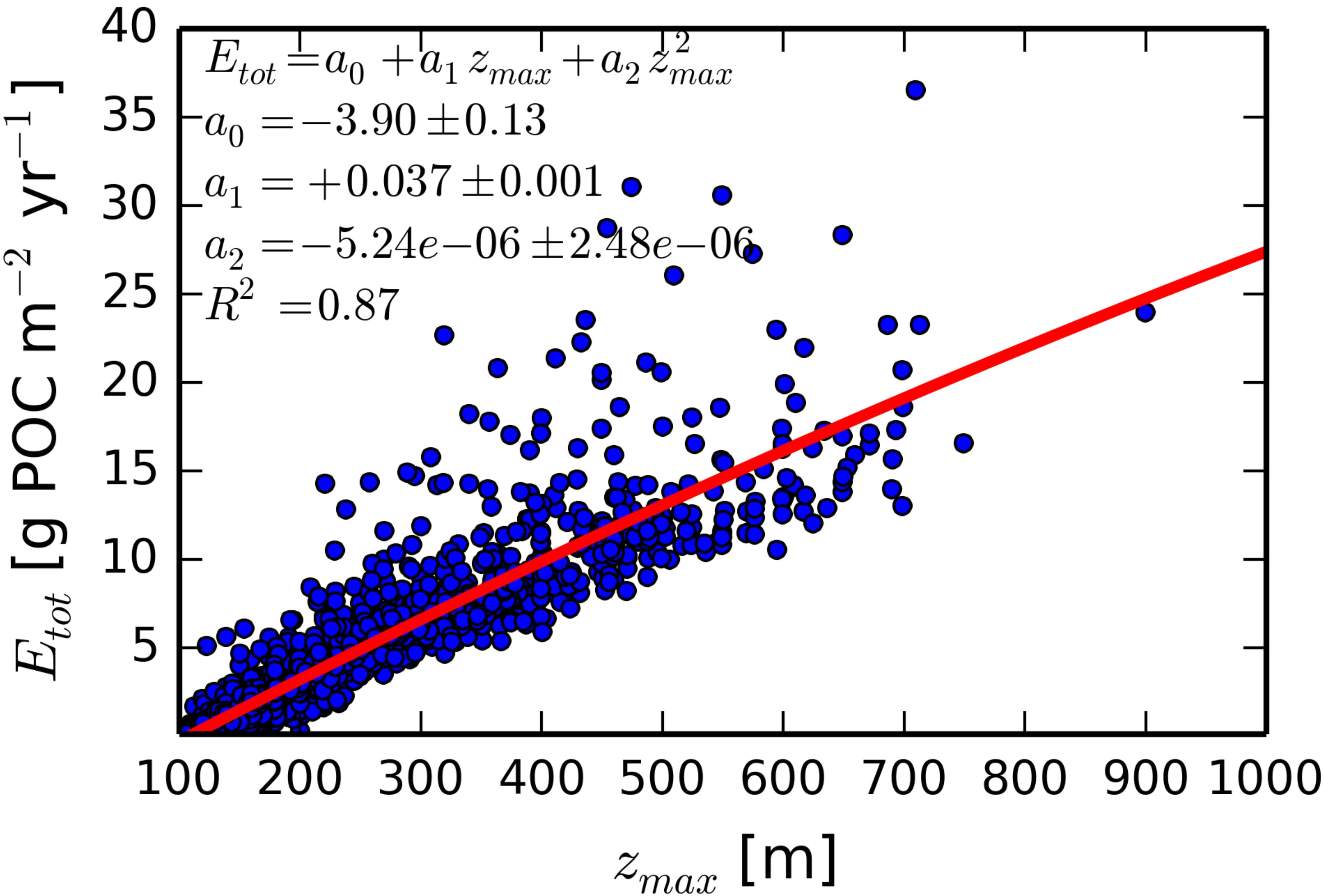

$E_{tot} = a_0 + a_1 z_{max} + a_2 z_{max}^2$
$a_0 = -3.90 \pm 0.13$
$a_1 = +0.037 \pm 0.001$
$a_2 = -5.24e-06 \pm 2.48e-06$
$R^2 = 0.87$
E_{tot} [g POC m^{-2} yr^{-1}]
z_{max} [m]
40
35
30
25
20
15
10
5
100
200
300
400
500
600
700
800
900
1000

Figure S5

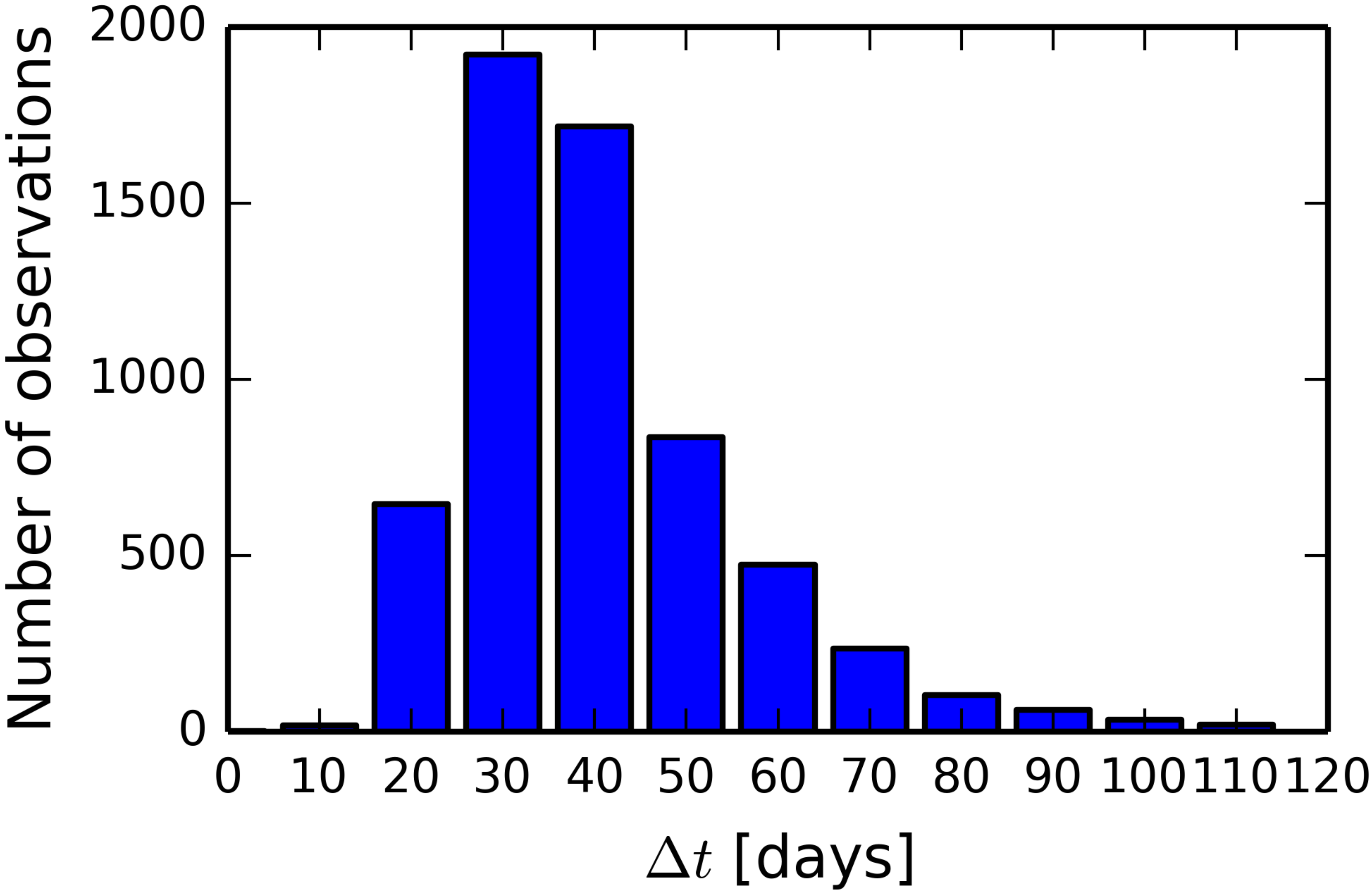
Number of observations
2000
1500
1000
500
0
0
10
20
30
40
50
60
70
80
90
100
110
120
Δt [days]

Figure S6

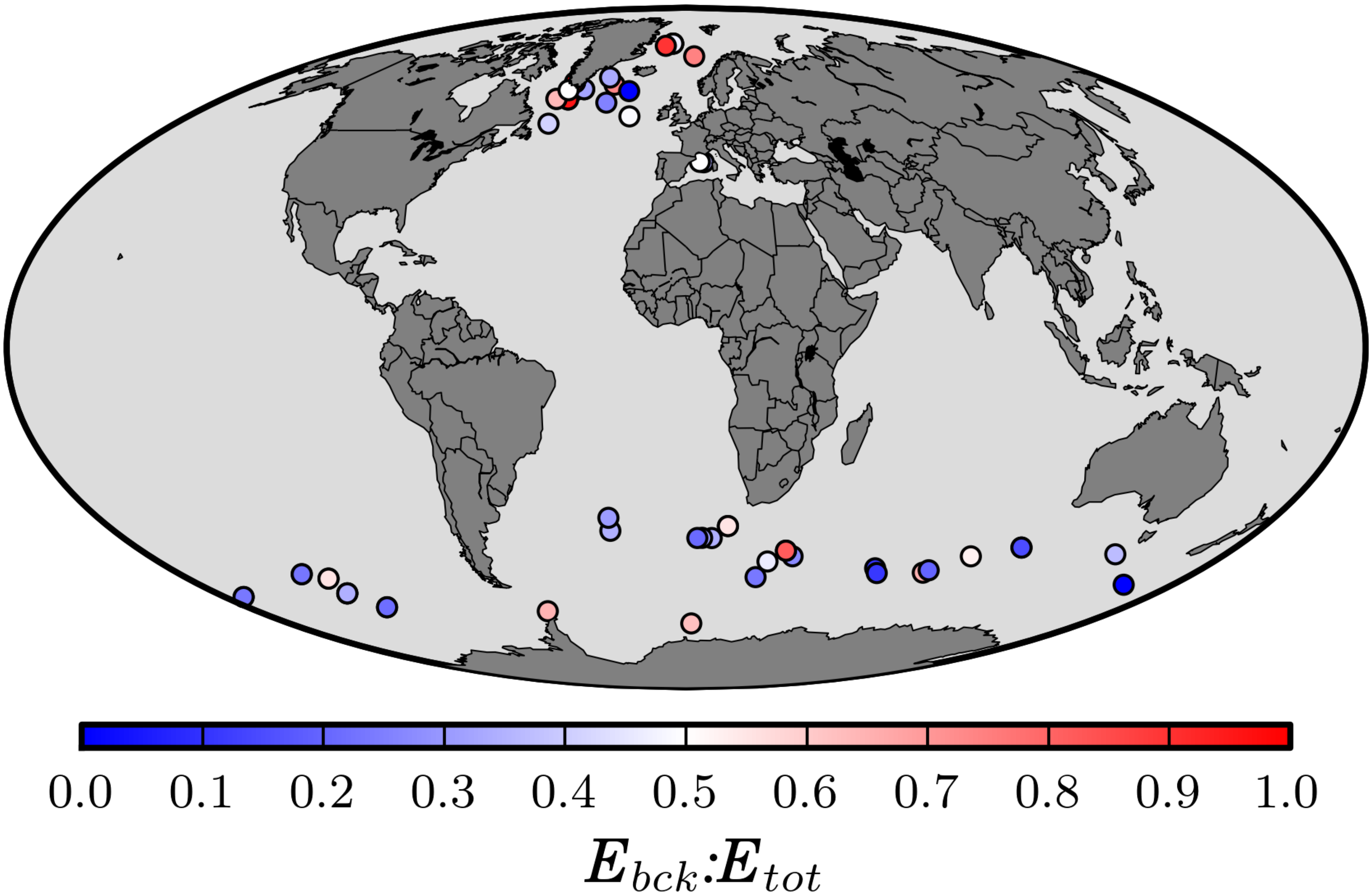

Figure S7